ADVANCED HEALTHCARE MATERIALS
www.advhealthmat.de

α-Galactosidase A Loaded Nanoliposomes with Enhanced Enzymatic Activity and Intracellular Penetration

Ingrid Cabrera, Ibane Abasolo, José L. Corchero, Elisa Elizondo, Pilar Rivera Gil, Evelyn Moreno, Jordi Faraudo, Santi Sala, Dolores Bueno, Elisabet González-Mira, Merche Rivas, Marta Melgarejo, Daniel Pulido, Fernando Albericio, Miriam Royo, Antonio Villaverde, Maria F. García-Parajo, Simó Schwartz Jr., Nora Ventosa, and Jaume Veciana**

Lysosomal storage disorders (LSD) are caused by lysosomal dysfunction usually as a consequence of deficiency of a single enzyme required for the metabolism of macromolecules, such as lipids, glycoproteins, and mucopolysaccharides. For instance, the lack of α-galactosidase A (GLA) activity in Fabry disease patients causes the accumulation of glycosphingolipids in the vasculature leading to multiple organ pathology. Enzyme replacement therapy, which is the most common treatment of LSD, exhibits several drawbacks mainly related to the instability and low efficacy of the exogenously administered therapeutic enzyme. In this work, the unprecedented increased enzymatic activity and intracellular penetration achieved by the association of a human recombinant GLA to nanoliposomes functionalized with Arginine-Glycine-Aspartic acid (RGD) peptides is reported. Moreover, these new GLA loaded nanoliposomes lead to a higher efficacy in the reduction of the GLA substrate named globotriasylceramide in a cellular model of Fabry disease, than that achieved by the same concentration of the free enzyme. The preparation of these new liposomal formulations by DELOS-SUSP, based on the depressurization of a CO_2-expanded liquid organic solution, shows the great potential of this CO_2-based methodology for the one-step production of protein-nanoliposome conjugates as bioactive nanomaterials with therapeutic interest.

1. Introduction

Fabry disease is an inherited failure of the glycosphingolipid metabolism due to a deficient lysosomal α-galactosidase A (GLA) activity.[1,2] This enzymatic deficiency causes progressive accumulation of the glycosphingolipid, globotriaosylceramide (Gb3), in vascular endothelial lysosomes of kidneys, heart, skin, and brain leading to multisystemic clinical symptoms.[3,4] First clinical signs occur during childhood and, over time, microvascular disease of the affected organs progresses leading to early death.[5] Vasculature is directly involved in the pathophysiology and progression of the Fabry disease[6] Indeed, endothelial cells are the most predominantly affected cell type in this disease[5] and targeting of endothelial cells seems to be reasonable approach to improve the treatment and life-expectancy

Dr. I. Cabrera, Dr. E. Elizondo, Dr. P. Rivera Gil, Dr. E. Moreno, Dr. J. Faraudo, Dr. S. Sala, D. Bueno, Dr. E. González-Mira, Dr. N. Ventosa, Prof. J. Veciana
Institut de Ciència de Materials de Barcelona (ICMAB-CSIC)
Campus Universitari de Bellaterra
08193 Cerdanyola del Vallès, Spain
E-mail: ventosa@icmab.es; vecianaj@icmab.es

Dr. I. Cabrera, Dr. I. Abasolo, Dr. J. L. Corchero, Dr. E. Elizondo, Dr. P. Rivera Gil, Dr. E. Moreno, Dr. S. Sala, D. Bueno, Dr. E. González-Mira, Dr. M. Melgarejo, Dr. D. Pulido, Prof. F. Albericio, Dr. M. Royo, Prof. A. Villaverde, Dr. S. Schwartz Jr., Dr. N. Ventosa, Prof. J. Veciana
Centro de Investigación Biomédica en Red–Bioingeniería Biomateriales y Nanomedicina (CIBER-BBN)
Spain

Dr. I. Abasolo, Dr. S. Schwartz Jr.
CIBBIM-Nanomedicine
Vall d'Hebron Institut de Recerca (VHIR)
Universitat Autònoma de Barcelona
08035 Barcelona, Spain

Dr. J. L. Corchero, Prof. A. Villaverde
Departament de Genètica i de Microbiologia
Institut de Biotecnologia i de Biomedicina
Universitat Autònoma de Barcelona
08193 Bellaterra, Spain

M. Rivas, Prof. M. F. García-Parajo
ICFO-Institut de Ciencies Fotoniques
Mediterranean Technology Park
08860 Castelldefels, Barcelona, Spain

Dr. M. Melgarejo, Dr. D. Pulido, Dr. M. Royo
Combinatorial Chemistry Unit
Barcelona Science Park
Baldiri Reixac 10, 08028 Barcelona, Spain

Prof. F. Albericio
Institute for Research in Biomedicine
Barcelona Science Park
08028 Barcelona, Spain

Prof. F. Albericio
Department of Organic Chemistry
University of Barcelona
08028 Barcelona, Spain

Prof. M. F. García-Parajo
ICREA-Institució Catalana de Recerca i Estudis Avançats
08010 Barcelona, Spain

DOI: 10.1002/adhm.201500746

of Fabry patients.[7] The current treatment, available since 2001, is the enzyme replacement therapy (ERT) in which a recombinant protein is administered intravenously to patients every other week. Two of such treatments are currently commercialized: agalsidase alfa (Replagal; Shire Human Genetic Therapies, Dublin, Ireland) and agalsidase beta (Fabrazyme; Genzyme Corporation, Cambridge, MA). Another chemically modified version of the recombinant α-galactosidase A protein is currently being tested in phase I/II clinical trials (PRX-102; Protalix Biotherapeutics, Carmiel, Israel).[8] GLA enzyme replacement therapy has demonstrated positive effects on clearing Gb3 from plasma and the target organs, reversing the pathogenesis of the disease.[9,10] However, this approach presents some disadvantages related to: (1) its limited efficacy in patients with an advanced stage of the disease, (2) short half-life of the enzyme mainly due to the sequestration of the enzyme by the liver, and (3) the high cost of the treatment (280.000 €/patient·year) due to the need for repeated administration of large amounts of enzyme.[4,11,12] For this reason, new treatment strategies are nowadays under investigation. For instance, in PRX-102, currently in clinical trials, GLA enzyme has been chemically modified with a homo-bifunctional polyethylene glycol (PEG, 2000 Da) cross-linker attached to the two protein subunits of the GLA enzyme, resulting in a PEGylated and covalently bound homo-dimer. This chemical modification of the enzyme, produced in a tobacco plant cell culture, is equivalent in functionality to the mammalian produced GLA, but vastly improves serum half-life as well as plasma and lysosomal stability. Gene therapy, chaperons or substrate reduction, constitute alternative therapies to ERT, which are at present under investigation.[13–16] The use of drug delivery systems represents a promising opportunity to enhance the efficacy of ERT. In this sense, nanotechnology offers a great availability of materials and strategies to build up the "perfect" nanocarrier for the precise and targeted delivery of therapeutic biomolecules, such as GLA used in ERT for Fabry disease. In this approach, in which the biomolecule is not chemically modified, the efficacy improvement is attained through its noncovalent assembling to a nanocarrier. For example, Giannotti et al. reported the formation of stable polyelectrolyte complexes between trimethyl chitosan and GLA, and their traffic to lysosomal compartments of human endothelial cells.[11] Polymeric nanoparticles coated with anti-ICAM-1 (an antibody expressed on endothelial cells and cells of the immune system) and loaded with GLA have also shown an increased endocytosis of the carrier by vascular endothelial cells as well as Gb3 degradation.[17] Unfortunately, most of these systems are metastable and tend to lose their colloidal stability with time.[18] Moreover, their physicochemical parameters change upon interaction with complex systems, such as the physiological media preventing their intravenous dosage, but also with the intracellular environment, which can affect the performance of the drug.[19,20] Therefore, critical parameters, such as chemical composition, size, geometry, charge, stability over time, and loading efficiency need to be carefully controlled and fixed during the preparation of GLA nanoconjugates. This is particularly crucial in order to establish a correlation between the structure of the nanocarrier and its biological effectiveness. Changes in the structuring of the carrier upon loading of the cargo molecule and/or upon formation of the protein corona have shown to directly affect cell internalization patterns and thus the efficiency of drug/enzyme release and its bioavailability.[21–23]

Recently, we have demonstrated the potential of the DELOS-SUSP method for the easy and direct preparation of different vesicle-biomolecule conjugates with nanoscopic size and great degree of unilamellarity.[24,25] This methodology, based on the use of compressed CO_2, shows a high "batch-to-batch" consistency allowing for the preparation of sufficient quantities (up to liter scale) of nanotherapeutics for clinical testing. Importantly, the bioactivity of the integrated molecules is unaffected under the mild processing conditions and their scale-up production is possible following GMP (Good Manufacturing Practices) requirements. Although liposomes, and in general lipid-based vesicles, are well recognized as useful and versatile drug carriers,[26–28] there is no previous reference of their use in the integration/encapsulation of GLA for the ERT of Fabry disease. In this work, we present a new promising liposomal nanomedicine candidate, capable of specific targeted delivery of the GLA enzyme to the lysosomes of endothelial cells. In this nanomedicine, GLA is conjugated to liposomes functionalized with an RGD targeting peptide.[25] On the one hand, the incorporation of this endothelial cell targeting peptide stabilizes the final liposomal formulation.[25,29] On the other hand, the RGD moiety allows for $\alpha v\beta 3$ integrin recognition, expressed in vascular endothelial cells,[30] which could promote a more specific and effective cellular uptake . Indeed, the use of receptor mediated internalization of the enzyme has been already described for the treatment of lysosomal storage disorder (LSD) either using chimeric proteins where the lysosomal enzyme has been fused to Tat or IGF II proteins,[31] or in nanoparticles where targeted delivery was mediated by anti-ICAM-1 antibodies.[17] As explained above, the targeting of the nanovesicles to the vascular endothelial cells is not spurious, since alterations in the vasculature are thought to be crucial in the pathophysiology of Fabry disease.[6] Moreover, the $\alpha v\beta 3$ integrin expression and urinary excretion has been already linked to the progression of the renal injury in Fabry disease.[32] Therefore, we envision that the use of RGD decorated liposomes carrying GLA would improve the efficacy of the current enzyme replacement therapy.

2. Results and Discussion

2.1. Preparation and Physicochemical Characterization of Nanoconjugates

2.1.1. Preparation

The recombinant human GLA used for the preparation of the conjugates was obtained by a transient gene expression-based production method[33] (Section 2, Supporting Information). Compared to the clinically approved versions of the GLA, our GLA contains an HIS-tag that permits its rapid an efficient purification, retaining 70% of the enzymatic activity of the clinically available proteins. Moreover, the use of this "in-house" version of GLA allowed us to control the buffer and media in which the enzyme is contained. Such additives are not quantitatively described for the clinical versions (Replagal and Fabrazyme)

DOI: 10.1002/adhm.201500746

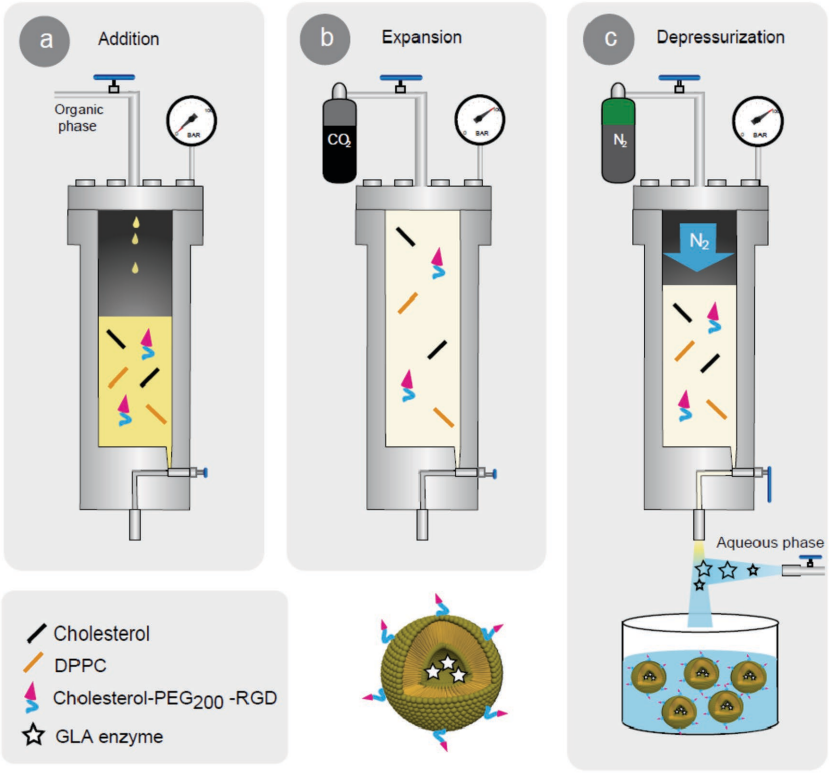

Figure 1. Schematic representation of the DELOS-SUSP method for the preparation of GLA loaded liposome-RGD conjugates. The procedure includes: a) Loading of an organic solution of the lipidic membrane components (Cholesterol, DPPC, and Cholesterol-PEG$_{200}$-RGD) into an autoclave at a working temperature (T_W = 308 K) and atmospheric pressure. b) Addition of compressed CO_2 to produce a CO_2-expanded solution, at X_{CO2} = 0.85, working pressure (P_W = 10 MPa), and T_W, where all membrane components remain dissolved. c) Depressurization of the expanded solution over an aqueous solution containing the free GLA enzyme, in order to produce the nanoconjugates.

and therefore their potential effect in the encapsulation of the protein cannot be excluded.

The enzyme loaded nanovesicles were prepared following the procedure schematically represented in **Figure 1** and described in Experimental Section. Briefly, an ethanolic solution containing cholesterol, 1, 2-dipalmitoyl-sn-glycero-3-phosphocholine (DPPC) and RGD peptide linked to cholesterol (cholesterol-PEG$_{200}$-RGD) in a molar ratio 6:10:1 was added to a small-scale reactor of 7.5 mL and pressurized with large amount of compressed CO_2. The nanoconjugates were formed by depressurizing the resulting CO_2-expanded solution of lipids over an aqueous solution containing the GLA enzyme at the desired concentration. Three different enzyme concentrations, 8.5, 20.0, and 42.5 μg mL^{-1}, were tested for the preparation of the liposomal systems. No further energy input was required for achieving the desired structural characteristics of GLA loaded liposome-RGD conjugates, neither for increasing the loading or the integration efficiencies. The composition of the organic and aqueous phases used for the preparation of the different GLA liposomal conjugates are given in Table S1 (Section 3, Supporting Information). The reasons for using the RGD peptide were two: (1) Cells affected by the Fabry disease show overexpression of integrins, which are ligands for RGD and (2) to take advantage of the integrin internalization pathway for the uptake of the nanoconjugates.[25]

2.1.2. Physicochemical Characterization

The particle size, polydispersity index (PdI), and ζ-potential of the resulting nanoconjugates were determined using a dynamic light scattering (DLS) equipment and are reported in **Table 1**. Although all the conjugates were in the nanoscale range, their average sizes (168, 216, and 226 nm) and polydispersity were influenced by the GLA concentration in the liposomal system (8.5, 20.0, and 42.5 μg mL^{-1}). Thus, the higher the enzyme concentration the larger the particle size. In addition, ζ-potential values, which are indicators of the colloidal stability, showed a dependence on the enzyme concentration. In theory, higher ζ-potential values, being positive or negative, correspond to more stable colloidal systems. Usually particle aggregation is less likely to occur for charged particles with pronounced ζ-potential values due to the electrostatic repulsion between particles with the same electrical charge. Accordingly, systems containing 8.5 μg mL^{-1} of the enzyme showed the highest ζ-potential value (+18.0 mV) and were stable for at least two months (see Section 4.1 of the Supporting Information), whereas liposomal systems with 42.5 μg mL^{-1} and with the lowest ζ-potential value (+9.4 mV), presented a slight phase separation within the first 15 d after their preparation. Nevertheless, after a diafiltration procedure to separate the nonloaded enzyme from the aqueous dispersion of GLA loaded nanoliposomes, all the ζ-potential values changed from positive to negative (≤–25 mV), explaining the increase in stability observed.

These results indicate that there is a tendency toward less homogeneous and less stable liposomal systems when increasing the enzymatic concentration. This behavior was observed not only when the dispersant medium was pure mQ water, but also in physiological media, such as several physiological buffers or even in cell culture media, which is a water-based solution containing mainly serum proteins and with a relatively high ionic strength (see Section 4.2 of the Supporting Information). The composition of the vesicular membrane of all nanoconjugates described in Table 1 is exactly the same; therefore we can conclude that the incorporation of the cargo molecule, the GLA enzyme, is the main reason for the alteration of the nanocarrier's structure and thus, their physicochemical properties. Next, we quantified the amount of incorporated enzyme in the GLA loaded liposome-RGD conjugates. For this, the nonloaded GLA was separated from the loaded vesicles by a diafiltration process (Section 5, Supporting Information). The total sample and the loaded vesicles were analyzed by SDS-PAGE and further Western blot

Table 1. Physicochemical characteristics, entrapment efficiencies (EE), and loading of nanoliposome conjugates. The physicochemical characteristics of the conjugates after the separation of the nonloaded enzyme are given between brackets.

Liposomal systems (initial GLA concentration)	Size		ζ-potential [mV]	EE [%]	GLA loading[c] [μg mg^{-1}]	GLA concentration[d] [μg mL^{-1}]	GLA's/lip[e]
	Mean[a][49]	PdI[b]					
GLA loaded liposomes-RGD (8.5 μg mL^{-1})	168 ± 1 (146 ± 1)	0.33 ± 0.01 (0.29 ± 0.03)	18 ± 1 (–33 ± 1)	39 ± 10	(2.3 ± 0.6)	8.5 (3 ± 1)	1
GLA loaded liposomes-RGD (20.0 μg mL^{-1})	216 ± 8 (195 ± 1)	0.40 ± 0.01 (0.40 ± 0.01)	14 ± 1 (–24 ± 2)	37 ± 9	(5.8 ± 1.3)	20 (7 ± 2)	3
GLA loaded liposomes-RGD (42.5 μg mL^{-1})	226 ± 3 (215 ± 6)	0.45 ± 0.04 (0.33 ± 0.02)	9.8 ± 0.4 (–32 ± 1)	38 ± 8	(11.3 ± 2.3)	42.5 (16 ± 3)	4
Liposomes-RGD/water (blank)	160 ± 1	0.38 ± 0.02	30 ± 2	–	–	–	–
Plain liposomes (without RGD)	149 ± 2	0.20 ± 0.01	3.5 ± 0.2	–	–	–	–
GLA loaded plain liposomes (20 μg mL^{-1})	158 ± 3 (182 ± 4)	0.18 ± 0.01 (0.40 ± 0.01)	5.97 ± 0.09 (–12.7 ± 0.3)	33 ± 11	(4.6 ± 1.5)	20 (7 ± 2)	3

[a]Intensity weighted mean hydrodynamic size (diameter) measured by dynamic light scattering; [b]Polidispersity index showing the width of the particle size distribution; [c]Mass of the integrated enzyme (determined by Western blot), divided by the total mass of the membrane components forming the vesicles; [d]Mass of enzyme present divided by the volume of the vesicular suspension. Error margins are SD; [e]Number of GLA molecules per nanoliposome.

and the entrapment efficiency (EE) was calculated dividing the mass of integrated enzyme by the total initial mass used in the experiment (Table 1). EE values of ≈40 ± 10% were obtained in all cases. Hence, liposomal systems free of nonconjugated enzyme with 3, 7, and 16 μg mL^{-1} of GLA concentration, were obtained, respectively, by diafiltration of the original liposomal systems with 8.5, 20.0, and 42.5 μg mL^{-1} of GLA concentration. As it can be seen in Table 1, GLA loading of nanoconjugates increases with the increase of GLA concentration of the liposomal system. Even when the enzyme loadings were not very high, the effectiveness of the integrated GLA was improved compared to the free enzyme as we will show below. As detailed in the Supporting Information, the loaded nanoconjugates were able to retain 84% of the initial encapsulated GLA after 21 d stored at 4 °C (Section 6, Supporting Information).

Finally, for liposomal system free of nonconjugated enzyme with a 7 μg mL^{-1} of GLA concentration, we estimated the ratio between GLA adsorbed on the outside surface of the liposomes and GLA encapsulated in the liposome. To do this estimation, a new sample, named as "Liposome-RGD + Free GLA + Diafiltration", was prepared by incubating empty liposomes-RGD (see Table S1 of the Supporting Information) with free GLA at a concentration of 20 μg mL^{-1} during 24 h, followed by a diafiltration process to take out the GLA nonadsorbed on the bilayer. SDS-PAGE and further Western-blot analysis (Experimental Section) revealed that this sample had a GLA concentration of 3.5 ± 0.8 μg mL^{-1}. Theoretical MD simulations, reported later on in this paper, show that GLA is incorporated in the membrane as a peripheral protein. Therefore, it is worthy to suppose that all GLA of this new liposomal system is adsorbed on the outside surface of the bilayer and that no entrapped GLA is present. By the comparison of the above described liposomal systems, a ratio of "GLA adsorbed/GLA encapsulated" close to 1 can be estimated for the liposomal system free of nonconjugated enzyme with a 7 μg mL^{-1} of GLA concentration.

Figure 2 clearly shows how the amount of loaded enzyme influences the final morphology of the nanoconjugates. When there is no protein loaded, spherical and unilamellar vesicles are observed by direct inspection with cryo-TEM and by averaged structural characterization with SAXS (see Section 15.3 of the Supporting Information). This morphology changes toward more polydisperse oligolamellar systems with GLA loading. At 16 μg mL^{-1} GLA concentration, the increase in broadness of the SAXS curve indicates a higher polydispersion in the interbilayer distance in comparison to less GLA loaded nanoconjugates. Indeed it is described that biomolecules may induce phase transformations, free energy releases, restructuring, and dissolution at the nanomaterial surfaces.[34]

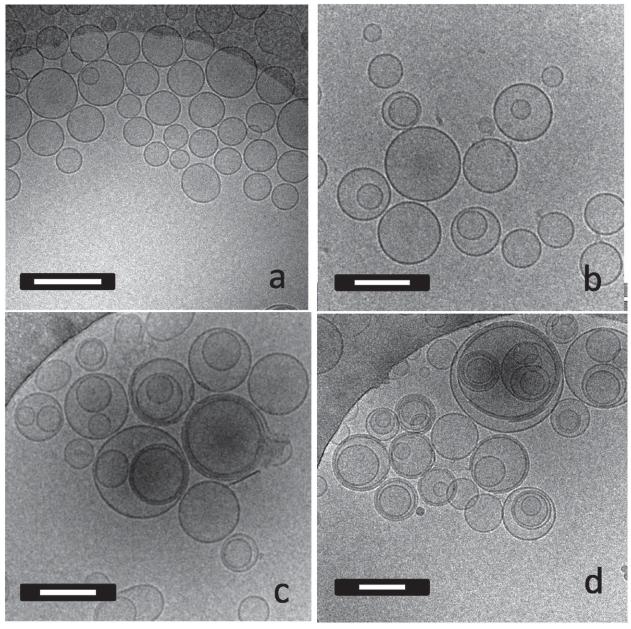

Figure 2. Cryo-TEM pictures showing the morphology of the nanoconjugates with different GLA concentrations. a) Unloaded liposomes-RGD, b) GLA loaded liposome-RGD conjugates containing 3 μg mL^{-1} of GLA, c) GLA loaded liposome-RGD conjugates containing 7 μg mL^{-1} of GLA, d) GLA loaded liposome-RGD conjugates containing 16 μg mL^{-1} of GLA enzyme. Scale bars are 200 nm.

Table 2. Specific enzymatic activities (in μmol 4-MU mg^{-1} GLA h^{-1}) of GLA liposomal systems.

Liposomal systems (initial GLA concentration)	Total[a)]	GLA loaded liposomes[b)]	Free GLA in water[c)]
GLA loaded liposomes-RGD (8.5 μg mL^{-1})	913 ± 27	924 ± 89	304 ± 14
GLA loaded liposomes-RGD (20 μg mL^{-1})	846 ± 270	1253 ± 65	400 ± 49
GLA loaded liposomes-RGD (42.5 μg mL^{-1})	879 ± 140	705 ± 88	548 ± 200
Unloaded liposomes-RGD	0	0	0

[a)]Total GLA, corresponding to the fraction prior diafiltration in which the nonloaded and the liposome loaded GLA coexist together; [b)]GLA loaded nanoliposomes, corresponding to the fraction obtained after the diafiltration process; [c)]free GLA, corresponding to the initial GLA aqueous solution before its conjugation. Error margins are SEM.

2.1.3. Specific Enzymatic Activity of Free versus Conjugated GLA

The preservation of the specific enzymatic activity of GLA, which is the enzyme activity per milligram of total enzyme, after the entrapment process was subsequently measured (Experimental Section). To this end, free and conjugated GLA were incubated with a nonfluorescent substrate (4-MUG) that after GLA cleavage renders a fluorescent product (4-MU). By measuring the increase of the fluorescence signal upon enzymatic hydrolysis of the substrate, we could establish the specific activity of GLA in its different forms. As it could be observed in **Table 2**, unloaded liposome-RGD do not give any fluorescence signal, showing that these liposomal carriers do not affect the enzymatic assay. We studied the three following samples for comparison: (i) free GLA in water withdrawn from the aqueous phase used in the experiments, (ii) GLA loaded liposomes obtained after the diafiltration process, and (iii) total GLA, corresponding to the fraction prior diafiltration in which the nonloaded and the liposome-integrated GLA coexist together. Table 2 shows the specific enzymatic activity values for such samples. Remarkably, the specific activity of the GLA always increases when it is conjugated to the liposomes. In the liposomal systems with 8.5 and 20 μg mL^{-1} GLA concentrations, it was observed a significant specific activity increase when nonconjugated GLA was separated by diafiltration. **Figure 3**A shows the ratio between the specific enzymatic activities of the GLA loaded nanoconjugates and of the free GLA. The increment in the specific activity is 3-fold for the nanoconjugates with 3 and 7 μg mL^{-1} GLA concentration, but reduces to 1.3-fold for the conjugate with 16 μg mL^{-1} GLA content. To the best of our knowledge, such increase of the activity of the enzyme after its conjugation to liposomes has not been observed before.

In order to discard the influence of CO_2 or ethanol in this activity enhancement, the specific activity of GLA was also measured in a sample obtained by depressurizing CO_2-expanded ethanol free of lipids over a water solution containing the enzyme at concentration of 8.5 μg mL^{-1}. The resulting specific activity was similar to that obtained for the GLA in water without any treatment. This result indicates that the activity enhancement is related to the enzyme-liposome association (Section 7, Supporting Information). A similar increment in specific activity for GLA was recently reported by Corchero et al. when GLA was immobilized on the surface of magnetic particles.[35] This enhancement was related to the covalent anchoring of the enzyme with a "site-specific" oriented manner. This explanation could also apply for our liposomes, since the GLA may be interacting directly with the lipid bilayer immobilizing the enzyme. Indeed, immunomicroscopy images show the presence of the enzyme in the membrane of nanovesicles (see Section 8 of the Supporting Information). Although GLA is not covalently bound, other kind of interactions (i.e., electrostatic and/or hydrophobic) between the enzyme and the lipid membrane components may ensure enzyme immobilization. This

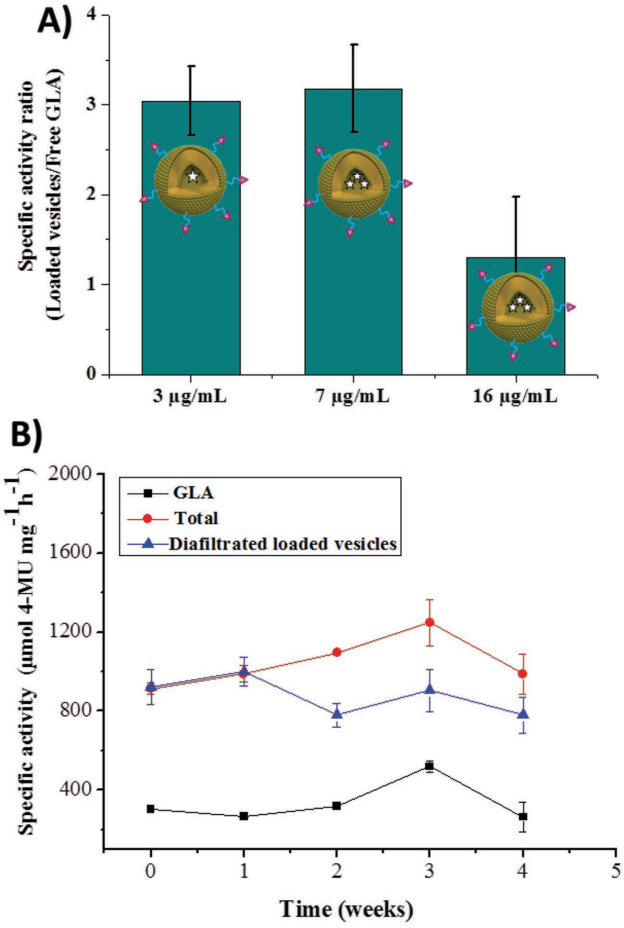

Figure 3. A) Ratio between the specific enzymatic activity of the GLA loaded nanoconjugates and of the free GLA in water for different enzyme concentrations. B) Evolution of the specific enzymatic activity of the free GLA, GLA loaded liposome-RGD conjugates plus nonloaded GLA (Total), and GLA loaded liposomes-RGD after the elimination of the nonloaded GLA by diafiltration, corresponding to the liposomal system with a GLA initial concentration of 8.5 μg mL^{-1} (see Table 1). Samples were stored at 4 °C during the time of analysis. Represented values correspond to mean ± SEM.

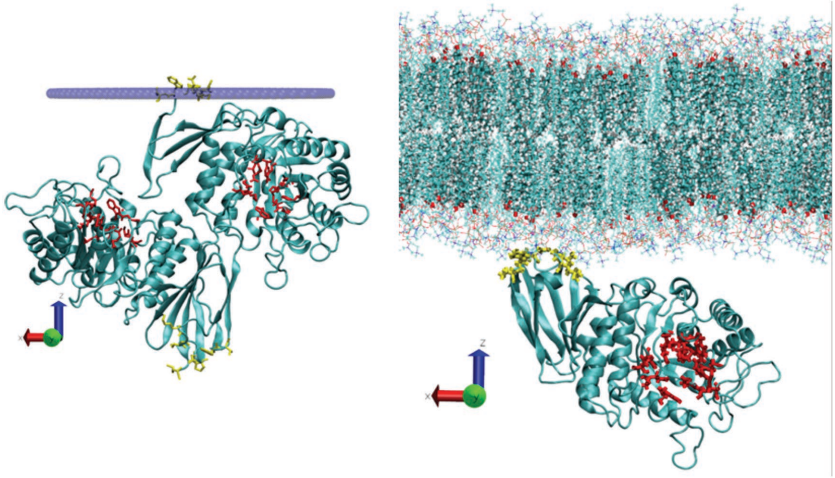

Figure 4. Results for the atomistic modeling of the interaction between GLA and a DPPC/Chol bilayer. The protein residues involved in the interaction with the membrane are shown as yellow bonds and the residues involved in the active enzymatic region are shown as red bonds. Left: Equilibrium configuration of the protein dimer obtained from the approximate thermodynamic calculation. The boundary of the hypothetical membrane is shown in blue. Right: Snapshot of a particular configuration obtained in MD simulations of monomer and a DPPC/Chol bilayer. The lipids are shown as lines. The cholesterol molecules inside the membrane are emphasized. All images were produced using VMD.[48]

in turn might be responsible for the increased activity. Other examples of enhanced enzymatic activity with nanoparticle bioconjugates, mainly using inorganic nanoparticles, have also been discussed by Brandy J. Johnson et al., when compared to freely diffusing enzyme in bulk solution.[36]

In order to confirm our hypothesis, we performed a theoretical analysis with atomistic resolution, of the interaction of the GLA protein with the bilayer. Our modeling of the protein employs the X-ray structure determined by Garman et al.[37] The analysis was made using two different techniques, the thermodynamic technique described by Lomize et al.[38] and large-scale atomic molecular dynamics simulations.

First, we determined the preferred orientation and positioning of the protein, relative to a bilayer, using the fast and accurate thermodynamic methodology described in Lomize et al.[38] We obtained that GLA dimer is incorporated as a peripheral protein, with only eight residues of a single monomer embedded in the bilayer and an overall tilt angle of 70 ± 10° (**Figure 4**). These residues are LYS374, GLY375, VAL376, ASN379, PRO380, TRP399, THR400, MET421, which are located in the second domain of the monomer. The active site of the protein is found in the first domain (see Figure 2 in Garman et al.[37]), at about 2.6 nm from the bilayer. The free energy of transfer estimated from the thermodynamic method is -6 kcal mol^{-1}.

Although in general the thermodynamic calculation is accurate for protein–bilayer interactions,[38] it has limitations. In particular, it considers the full structural detail of the protein but considers only implicitly the solvent (water) and the membrane. In fact, the model for the membrane is so generic that the composition of the bilayer is neglected. In order to refine our calculations, we have confirmed the results of the simplified thermodynamic model by performing large-scale molecular dynamics simulations under conditions of 1 atm, 25 °C and pH = 7. In our simulations, we considered the interaction of GLA with a fully hydrated membrane patch containing DPPC and cholesterol with a 10:6 molar ratio, representative of the experimental situation. Since our previous thermodynamic calculation shows that only one monomer of the dimer interacts with the bilayer, we have performed our simulations considering only one monomer of the protein. In spite of this simplification, the simulation box contains more than 10^5 atoms, a substantial amount which requires the use of supercomputing facilities. Full technical details of the simulations are given in the Supporting Information (Section 16).

The results obtained from the MD simulations confirm that only the residues identified by the thermodynamic method (located in the second domain) are responsible for the interaction with the DPPC/Cholesterol bilayer, so the active center is located far from the membrane. In our MD simulations, these residues do not fully penetrate inside the bilayer. Rather, they are typically surrounded by choline lipid head groups. We do not observe direct binding between atoms of these protein residues and atoms in the DPPC lipids (hydrogen bonds or other). In fact, the distance between closest protein and DPPC atoms is always larger than 0.25 nm. It has to be emphasized also that positioning of the protein at the membrane does not alter its structural features. The RMSD of the protein during the trajectory is only 1 Å taking as a reference structure the initial (unbound) protein.

Overall, our calculations suggest that the GLA protein is incorporated onto the nanocarriers adsorbing its second domain at the bilayer surface, as a peripheral protein, without modification of its structure. The adsorbed protein has its first domain oriented with the active site exposed toward the aqueous phase (opposite to the bilayer). This particular orientation of the immobilized protein, which is favorable for the protein enzymatic activity, also suggests that its adsorption at a surface can lead to an increased activity, as observed experimentally.

Additionally, the theoretical results described above could also explain the smaller specific activity increase observed for the conjugates with the highest GLA loading (Figure 3A). Indeed, less loaded liposomes showed a more homogeneous morphology regarding size and interbilayer distance. On the contrary, nanoconjugates with a higher loading (16 μg mL^{-1} in GLA concentration) showed a higher morphological polydispersity. The increase in oligolamellarity and polydispersion reduce access of the enzyme to the media, hindering its availability to metabolize the substrate and explaining its lower performance. Certainly, this issue requires and deserves further and deeper analysis. Nevertheless two phenomena appeared to have a decisive role in the observed increased activity upon integration: firstly, a possible immobilization of the enzyme at the lipid bilayer and secondly, the availability of the enzyme to the

Adv. Healthcare Mater. **2016**,
DOI: 10.1002/adhm.201500746

substrate due to a more homogeneous and unilamellar vesicle structures.

The stability of the entrapped GLA enzyme, during four weeks period, was further studied by measuring the specific activity in samples with free and entrapped GLA, corresponding to the liposomal system with initial GLA concentration of 8.5 μg mL^{-1} (Figure 3B). Neither the activity of the free GLA in water nor the activity of the enzyme associated to the liposomes was affected after one month. Although no differences in stability were found between the free and the encapsulated enzyme along time, a higher specific activity was present in the fractions in which the GLA was associated to vesicles compared to the free enzyme and remained unchanged during the four weeks. The specific activity was also measured after 14 weeks in samples were the enzyme was associated to the liposomes—both in samples without nonloaded enzyme and with it—and around 70% of the initial activity still remained in the formulation (Section 9, Supporting Information).

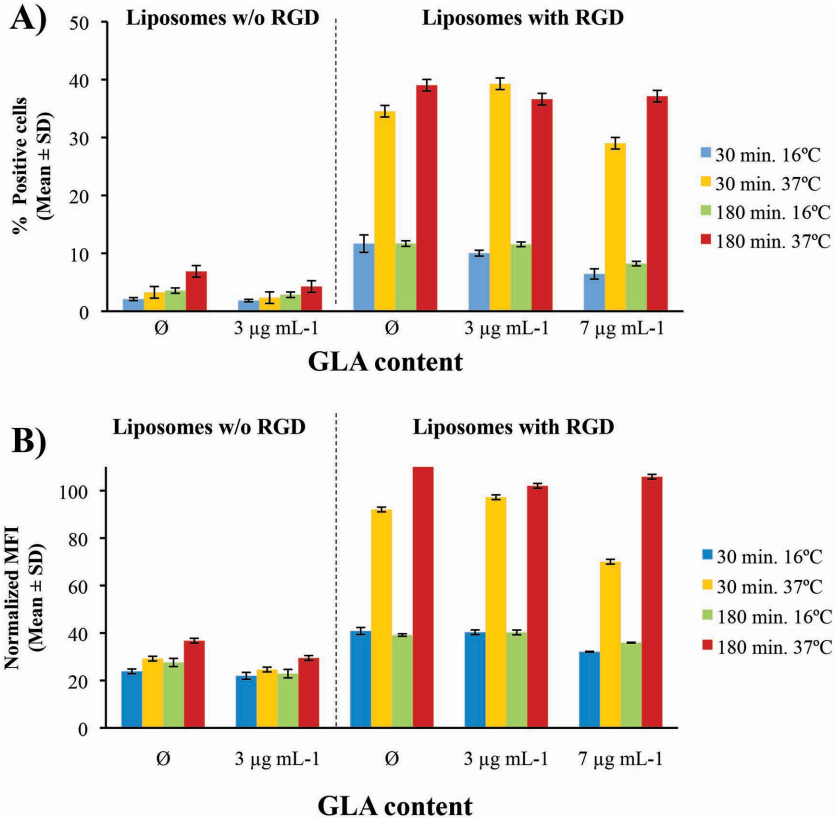

Figure 5. Internalization of nanovesicles on endothelial cells assessed by flow cytometry after 30 and 180 min of incubation at 16 °C and 37 °C: A) Flow cytometry quantification of the fraction of cells that internalized plain liposomes and liposome-RGD conjugates as the percentage (%) of DiD-positive cells among the total number of cells. B) Mean fluorescence intensity (MFI) of DiD in the cells normalized to the maximum fluorescence intensity. Blue and green bars correspond to cells incubated at 16 °C and refer to the liposomes bound to the membrane but not internalized, since active internalization is inhibited at this temperature. Comparatively, yellow and red bars corresponding to cells incubated at 37 °C, have significantly higher values only in the case of RGD-containing liposomes, indicating that the presence of the RGD moiety is essential for a fast and specific internalization of the liposomes.

2.1.4. Biological Characterization of Nanoconjugates

Cytotoxicity, Hemocompatibility, and Sterility Assays: For the biological characterization of nanoconjugates, we selected the less loaded RGD-functionalized liposomes (i.e., with 3 μg mL^{-1} of GLA) due to their superior colloidal stability. Such experiments were carried out on HeLa (cervix adenocarcinoma) and HMEC-1 cells (human microvascular endothelial cell line, obtained from Centers for Disease Control and Prevention/National Center for Infectious Diseases (CDC-NIDR)). Both types of cells were incubated with plain liposomes (non-RGD functionalized liposomes), unloaded liposomes-RGD, and with GLA loaded liposomes-RGD. Cell viability of both cell lines was not affected after 72 h (Section 10, Supporting Information) showing the lack of cytotoxicity of nanoconjugates in the range of concentrations tested. The three kinds of liposomes were also nonhemolytic, presenting a hemolytic percentage always under 2% (Section 11, Supporting Information), and sterile (Section 12, Supporting Information).

Cellular Internalization: Functionalization of colloids with RGD peptides is a common strategy to facilitate/accelerate their internalization by cells *via* integrin receptors recognition.[39–41] In our previous work, we demonstrated that liposomes-RGD, with the same membrane lipid composition used in the present work, showed 30-fold higher uptake by HMEC-1 cells than plain liposomes not functionalized with RGD, but with a similar cholesterol:DPPC molar ratio, the same DPPC concentration and prepared following the same CO_2-based procedure.[25] Here, we studied the internalization of RGD-functionalized nanoliposomes loaded with GLA at two different enzyme concentrations (i.e., 3 and 7 μg mL^{-1}) in order to see if the slight differences in the chemical structuring of the nanocarriers could interfere with their uptake by living cells. As controls, GLA loaded plain liposomes at the enzyme concentration of 7 μg mL^{-1}, as well as unloaded liposomes with and without RGD functionalization were also evaluated. For the flow cytometry assays, HMEC-1 cells (known to overexpress $\alpha v\beta 3$ integrins necessary for RGD targeting)[30] were incubated during 30 and 180 min at 16 °C and 37 °C with 0.3 mg mL^{-1} DiD-labeled liposomes (plain liposomes, GLA loaded plain liposomes, unloaded liposomes-RGD, and GLA-loaded liposomes-RGD with the two aforementioned enzyme concentrations). In agreement with our previous data,[25] these results reflected that cellular uptake of the liposomes was enhanced with the presence of the RGD, regardless the presence of the GLA. Moreover, as it is clearly observed in **Figure 5** the internalization is not significantly affected by the different GLA loading of liposomes-RGD. Indeed, unloaded liposomes-RGD and GLA loaded

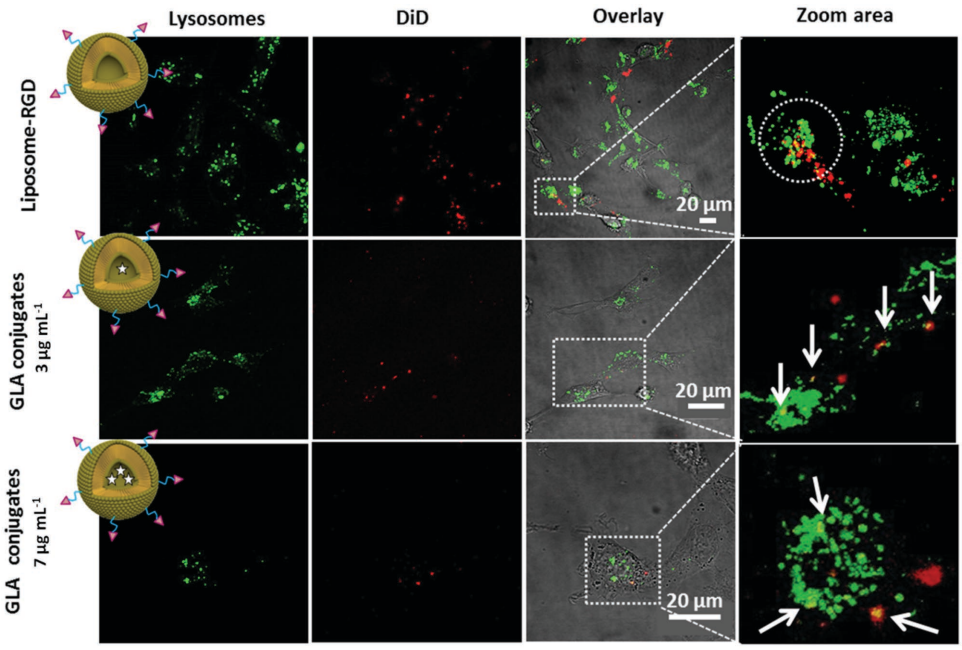

Figure 6. Confocal images of the cellular uptake of GLA-loaded liposome-RGD conjugates and unloaded liposome-RGD conjugates after 3 h incubation at 37 °C. The arrows denote the sites of colocalization between the labeled conjugates and the lysosomes.

liposomes-RGD at two different enzyme concentrations (i.e., 3 and 7 μg mL^{-1}), show the same internalization rate at 180 min at 37 °C, regardless that the number of GLA's per nanoliposome is 0, 1, and 3, respectively (see Table 1).

As it can be observed in Figure 5, after 180 min of incubation, 38 ± 1% of the cells exhibited internalization of DiD-labeled liposome-RGD conjugates at 37 °C, whereas this percentage was kept at 6 ± 2% for cells incubated with unloaded and GLA-loaded DiD-labeled plain liposomes, without RGD targeting. Furthermore, a decrease in the fraction of positive cells was observed for all the formulations when cells were incubated with the DiD-labeled samples at 16 °C, a temperature that reduces the endocytosis and, thus, allows determining the percentage of vesicles that bind to the cell membrane non-specifically (Figure 5A). When the mean fluorescence intensity (MFI) associated to the cells that have internalized the DiD-labeled liposomes was quantified (Experimental Section), significantly higher MFI values were obtained for the cells incubated with DiD-labeled liposome-RGD conjugates (Figure 5B). Although initially the internalization kinetics of the GLA-loaded liposomes-RGD conjugates was slower when the enzyme loading was higher, after 180 min the uptake of both systems was almost the same.

The results were also confirmed by laser scanning confocal microscopy (LCSM). For this assay, HMEC-1 cells were incubated for 180 min at 37 °C to induce internalization, with 0.3 mg mL^{-1} DiD-labeled liposomes, and stained with Lysotracker Green (Experimental Section; Section 13, Supporting Information). Confocal images depicted that all RGD-functionalized liposomes (loaded or unloaded) had already entered the cells after 180 min incubation and were localized within lysosomes (**Figure 6**). Therefore, this strategy ensures the release of the cargo at the right target organelle via RGD-integrin binding. Other alternative targeting moieties such as Tat peptide, IGF-II or anti-ICAM-1 have been described as a way to improve the biodistribution of the therapeutic enzyme, and in turn, increase the overall efficacy of ERT.[16,42,43]

In Vitro Enzymatic Efficacy: The ability of the GLA delivered by the liposome-RGD conjugates to reduce Gb3 deposits was tested in a cellular model of Fabry disease. To this end, GLA knock out (KO) mouse aortic endothelial cells (MAEC) were cultured and the capacity of different GLA loaded liposome-RGD conjugates formulations to metabolize its substrate (Gb3) was investigated by means of flow cytometry (Experimental Section). MAECs have been described to overexpress $\alpha v\beta 3$ integrins.[30] **Figure 7** shows the effect in the Gb3 loss for the formulations containing: (a) free GLA in water, (b) GLA loaded liposome-RGD conjugates plus nonloaded GLA (Total GLA), and (c) only GLA loaded liposome-RGD conjugates (Loaded GLA), corresponding to liposomal system with initial GLA concentration of 20 μg mL^{-1} (Table 1). The latter two samples produced a Gb3 loss better than the free enzyme, a result which is in agreement with the higher specific activity measured for these samples. This result was attributed to the conjugation of GLA to the nanoliposomes, since as depicted in Figure 7, empty liposome-RGD did not show any capacity to reduce Gb3 deposits.

In order to shed some light on the understanding of why the combination of free enzyme and liposome-loaded GLA (Total GLA) has a considerably better performance reducing lysosomal Gb3 deposits than the formulation containing only GLA loaded liposomes free of nonloaded enzyme (Loaded GLA), the capacity of two additional liposomal systems to clear Gb3 was also investigated. Formulation named as "Loaded GLA+Free GLA" was prepared by mixing the sample labeled as "Loaded GLA" (free of unloaded enzyme and with an enzyme

Adv. Healthcare Mater. **2016**,
DOI: 10.1002/adhm.201500746

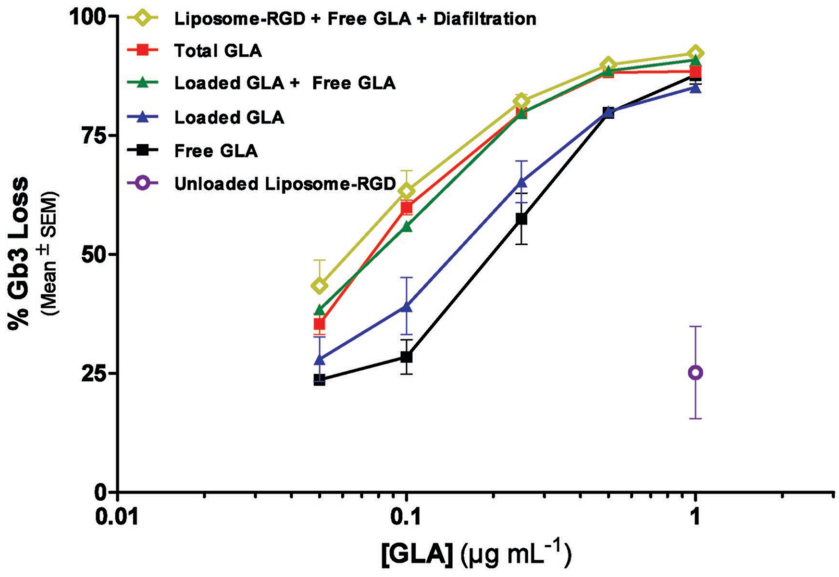

Figure 7. Effect of different formulations of GLA in the reduction of Gb3 deposits in aortic endothelial cells of Fabry KO mice. The activity of free GLA is compared to that of GLA loaded liposome-RGD conjugates containing nonloaded GLA (Total GLA), GLA loaded liposomes-RGD after the elimination of the nonloaded GLA (Loaded GLA), GLA adsorbed on the outside membrane of liposome-RGD (Liposome-RGD + Free GLA + Diafiltration), Loaded GLA mixed with additional free GLA (Loaded GLA + Free GLA), and Unloaded Liposome-RGD. This last sample equals the concentration of lipids used for the Loaded GLA. For all the formulations it has been used the same GLA batch with an enzymatic activity of 519 μmol h^{-1} mg^{-1}. Represented values correspond to mean ± SEM value.

concentration of 7 μg mL^{-1}) with additional GLA to reach a GLA sample concentration of 20 μg mL^{-1}, equal to the GLA concentration of sample labeled as "Total GLA". Formulation labeled as "Liposome-RGD + Free GLA + Diafiltration", described before in Physicochemical Characterization Section, has all GLA adsorbed on the outside surface of the bilayer and no GLA protein is present inside the nanoliposome. As it can be observed in Figure 7, the sample "Loaded GLA+free GLA", which was prepared to artificially reproduce the "Total GLA" sample, shows exactly the same capacity to clear Gb3. This result confirms that the coexistence of GLA loaded liposomes with the free enzyme gives a better Gb3 clearance than GLA loaded liposomes alone (sample "Loaded GLA").

These results could be explained if it is recognized that we can distinguish among three different types of GLA: (a) Free GLA in water; (b) GLA immobilized on the outside surface of the liposome bilayer, and according to theoretical simulations, anchored with a "site-specific" orientation with the active site exposed to the aqueous phase (opposite to the bilayer); and (c) GLA encapsulated inside the nanoliposome with a reduced access to the media. According to their accessibility to the media, it is probable that the ability to metabolize Gb3 of the three types of GLA decreases from the first one to the third one. Assuming this analysis, the results depicted in Figure 7 can be easily understood. Indeed, sample "Liposome-RGD+Free GLA+diafiltration" contains only the most accessible GLA, which is the one adsorbed on the outside surface of the liposomes, explaining its higher ability to reduce Gb3 deposits, with a mean GLA concentration value to reduce Gb3 deposits to the 50% (IC50) of 0.062 ± 0.004 μmol h^{-1} mg^{-1}. Samples labeled as "Total GLA" and "Loaded GLA + Free GLA", have the same composition with the three types of GLA. It explains their equal capacity to clear Gb3 (IC50 = 0.078 ± 0.005 and IC50 = 0.078 ± 0.009 μmol h^{-1} mg^{-1}, respectively) and their slightly lower capacity to reduce Gb3 in comparison to the previous formulation, which contains only the most accessible GLA. Sample labeled as "Loaded GLA", is composed of the same amount of GLA adsorbed on the outside membrane of the liposomes and of GLA entrapped inside the liposomes, as the sample "Total GLA", but on the contrary, this sample is free of nonloaded GLA, which is expected to have a higher ability to metabolize Gb3 than the entrapped one. This explains why "Loaded GLA" has a lower capacity to reduce Gb3 (IC50 = 0.14 ± 0.01 μmol h^{-1} mg^{-1}) than "Total GLA". Finally, the slightly higher capacity to clear Gb3 of "Loaded GLA" than the free enzyme "GLA" can be explained by a much higher ability to clear Gb3 of GLA adsorbed on the outside membrane (sample "liposome-RGD+Free GLA+diafiltration", IC50 = 0.062 ± 0.004 μmol h^{-1} mg^{-1}) in comparison to the free enzyme ("GLA", IC50 = 0.19 ± 0.03 μmol h^{-1} mg^{-1}), which might compensate the effect of having a portion of the less active entrapped GLA in sample "Loaded GLA".

3. Conclusion

Multifunctional nanoconjugates, composed by liposomes functionalized with RGD peptides and encapsulating GLA, were successfully prepared using the DELOS-SUSP method. This methodology yields nanometric conjugates with entrapment efficiencies around 40% that were noncytotoxic, nonhemolytic, and sterile. In vitro behavior of the GLA nanoconjugates has shown to be extremely related to its physicochemical characteristics and morphology. This result confirms the great importance of controlling nanostructure and physicochemical properties of drug delivery systems, such as liposomal formulations.[44]

Specific enzymatic activity assays performed on GLA conjugates showed a significant increase in the values reported when the enzyme was conjugated to the nanoliposomes in comparison with the values obtained for free GLA. In vitro activity studies in GLA deficient cells showed that the GLA loaded conjugates were also able to reduce lysosomal Gb3 deposits more efficiently than the free enzyme, in agreement with the greater specific activity encountered. The reduction in the lysosomal accumulation of Gb3 indicates that (i) multifunctional liposomes are uptaken by GLA deficient cells, (ii) that such liposomes reach the lysosomal compartment, and (iii) that the cargo (GLA) is efficiently released so that the GLA activity in the cells is restored. Thus, GLA loaded liposome-RGD conjugates constitute a potential nanomedicine for improving

the enzymatic replacement therapy in Fabry disease[29] by increasing the endothelial targeting and the final efficacy of the recombinant enzyme.

4. Experimental Section

DELOS-SUSP Methodology for the Preparation of Nanoconjugates: For the nanoconjugates preparation, 1.2 mL of an ethanolic solution containing cholesterol, DPPC, and cholesterol-PEG_{200}-RGD at a molar ratio 6:10:1, was loaded into a 7.5 mL high-pressure vessel at atmospheric pressure and at the working temperature (*T*w = 308 K). The solution was then volumetrically expanded with compressed CO_2 until a molar fraction (X_{CO2}) of 0.85 was achieved, reaching a working pressure (*P*w) of 10 MPa. The system was kept at 308 K and 10 MPa for approximately 1 h to achieve a complete homogenization and to attain thermal equilibration. 20 min before the depressurization stage, the enzyme (kept all the time at –20 °C) was left at room temperature until defrost. Once defrost, a given volume of this solution was dissolved in 24 mL of mQ water to reach the desired enzyme concentration (8.5, 20, or 42.5 μg mL^{-1}). In order to form the nanoconjugates, the volumetric expanded organic phase was depressurized over the aqueous solution containing the GLA. In this step a flow of N_2 at the working pressure is used as a plunger to push down the CO_2-expanded solution from the vessel and to maintain a constant pressure of 10 MPa inside the vessel during depressurization. Average time per experiment was 2 h and the resulting suspensions of nanoconjugates were stored at 4 °C until characterization. Details of the equipment configuration are given in Section 14 of the Supporting Information. The experimental conditions used for the preparation of the organic and aqueous phases of each formulation are given in Table S1 (Section 3, Supporting Information). The average sizes, polydispersivities (PdI), and Z potentials of all nanoconjugates were measured using a dynamic light scattering analyzer, the particle concentration was measured by nanoparticle tracking analysis, the morphology was studied by Cryo-TEM and the vesicular structure was probed by synchrotron Small and Wide-Angle X-ray Scattering (SWAXS). (See more details in Section 15 of the Supporting Information.)

The production and physicochemical characterization of the nanoconjugates have been performed by the platform of Production of Biomaterials and Nanomaterials of the ICTS "NANBIOSIS", more specifically by the Biomaterial Processing and Nanostructuring Unit of the CIBER in Bioengineering, Biomaterials and Nanomedicine (CIBER-BBN)/Jesús Usón Minimally Invasive Surgery Center (CCMIJU)) at the Institut de Ciència de Materials de Barcelona (ICMAB-CSIC).

Determination of the Entrapment Efficiency Percentage and Loading: To estimate the incorporation of GLA into liposomes-RGD, samples containing free GLA in water, samples with nonloaded and entrapped enzyme (total), and samples with GLA loaded liposomes after diafiltration, were mixed with denaturing, loading buffer and analyzed by SDS-PAGE and Western blot, that was further developed using a rabbit polyclonal anti-GLA serum (Santa Cruz Biotechnology) and a goat anti-rabbit IgG HRP-conjugate (Bio-Rad Laboratories, Inc.) as a secondary antibody. Amounts of GLA within each of the three above mentioned samples were estimated by comparison with known amounts (usually ranging from 25 to 125 ng) of GLA, previously produced, purified, and quantified in-house. Samples to be quantitatively compared were run in the same gel and processed as a set. Densitometric analyses of the bands were performed with the Quantity One software (Bio-Rad Laboratories, Inc.). Percentage of encapsulated GLA was obtained by dividing the amounts of enzyme found in the loaded vesicles by the amount found in the total sample.

Specific Enzymatic Activity: GLA enzymatic activity was assayed fluorometrically as described by Desnick et al. with the modifications of Mayes et al.[45,46] Basically, it was assayed by using 4-Methylumbelliferyl α-D-galactopyranoside (4-MUG, M-7633 Sigma Chemical) as substrate, at a concentration of 2.46 mM in assay buffer (0.01 M acetic acid, pH 4.5). A typical assay reaction mixture contains 100 μL of substrate and 25 μL of the sample. Enzymatic reactions took place in agitation (tubes placed in a rotator, set at a rotation speed of 25 rpm), at 37 °C for 1 h, and were stopped with 1.25 mL of 0.2 M glycine-NaOH buffer (pH 10.4). The released product (4-methylumbelliferone or 4-MU) was determined by fluorescence measurement at 365 and 450 nm as excitation and emission wavelengths, respectively. Samples of commercial product 4-MU (M-1381, Sigma Chemical) ranging from 5 to 500 ng mL^{-1} in 0.2 M glycine-NaOH buffer, pH 10.4, were used to obtain a calibration curve in order to transform fluorescence readings into product 4-MU concentration. Enzymatic activity and specific enzymatic activities are expressed as "ng 4-MU mL^{-1} h^{-1}" and "μmol 4-MU mg^{-1} h^{-1}", respectively.

Flow Cytometry: HMEC-1 cells were detached using trypsin and incubated with DiD-labeled liposomes or DiD-labeled liposome-RGD conjugates (0.3 mg mL^{-1}) resuspended into MCDB 131 media supplemented with 10 mM L-glutamine for 30 and 180 min at 16 °C or 37 °C. No significant toxicity was observed after this short-term incubation. Cells were subsequently washed twice with Dulbecco's phosphate buffered saline (DPBS) solution and resuspended in cell culturing medium before subjecting to fluorescence-activated cell sorting analysis. Data acquisition and analysis was performed using FACScan (Beckton-Dickinson) and BD FACSDiva software. At least 10^4 viable cells were evaluated in each experiment.

Cellular Uptake of Nanoconjugates Assessed by Laser Scanning Confocal Microscopy (LSCM): HMEC-1 cells were seeded onto Fluorodish culture plates (World Precision Instruments, Sarasota, FL) at a density of 2×10^5 cells per plate and allowed to grow for 36–48 h. 50 μL of DiD-labeled liposomes or DiD-labeled liposome-RGD conjugates (1.5 mg mL^{-1}) were mixed with 200 μL MCDB 131 medium, added into the cells and incubated for 180 min at 37 °C in a humidified atmosphere with 5% CO_2. Subsequently, cells were washed with serum-free MCDB 131 and incubated at 37 °C for 5 min with Lysotracker Green DND-26 (50 nM, Molecular probes, Eugene, Oregon) to label the endosomal/lysosomal compartments. The nuclei in live cells were stained with Hoechst 33342 dye (Sigma). Cells were examined under an inverted Leica SP5 laser scanning confocal spectral microscope (Leica Microsystems Heidelberg GmbH, Mannheim, Germany) using a 60 × 1.42 NA oil immersion objective. To visualize two colors of fluorescence simultaneously, we used the 514 nm line from Argon laser for Lysotracker Green and the 630 nm line from a He–Ne laser for DiD.

In Vitro Cell Assays: Primary cultures of MAEC of GLA deficient mice (Gla^{tmKul1}) were isolated at the In vivo Experimentation Platform from CIBER-BBN and Vall d'Hebron Institute of Research (VHIR) following procedures previously described.[47] Endothelial origin of isolated cells was confirmed by CD105 staining. For activity assays, cells in passages 2–5 were seeded in 24 well plates and maintained at 37 °C and 5% of CO_2. Twenty four hours after seeding 8 μM of NBD-Gb3 (Matreya) was added to the cultures along with the specified concentrations of tested compounds (free GLA enzyme, GLA loaded liposomes-RGD, empty liposome-RGD, etc.). After 48 h incubation, cells were trypsinized and Gb3-NBD fluorescent signal was analyzed by flow cytometry (FacsCalibur, Beckton Dickinson) and FCS Express v4 software. To calculate the percentage of Gb3-NBD signal, fluorescent signal in control cells (without treatment) was established as 100% and the rest of the values were normalized accordingly. Since GLA activity reduces those Gb3 deposits, the percentage of Gb3 loss (%Gb3 loss = 100 – %Gb3-NBD signal) was used to plot the results. IC50 values were calculated using GraphPad Prism 5 software.

Supporting Information

Supporting Information is available from the Wiley Online Library or from the author.

Adv. Healthcare Mater. **2016**,
DOI: 10.1002/adhm.201500746

Acknowledgements

The authors acknowledge financial support from Instituto de Salud Carlos III, through "Acciones CIBER". The Networking Research Center on Bioengineering, Biomaterials and Nanomedicine (CIBER-BBN) is an initiative funded by the VI National R&D&I Plan 2008–2011, Iniciativa Ingenio 2010, Consolider Program, CIBER Actions and financed by the Instituto de Salud Carlos III with assistance from the European Regional Development Fund. The authors appreciate the financial support through the "Development of nanomedicines for enzymatic replacement therapy in Fabry disease" project, granted by the Fundació Marató TV3, BE-WELL (CTQ2013-40480-R) project granted by DGI (Spain), GenCat (2014-SGR-17) project financed by DGR (Catalunya), LIPOCELL project financed by CIBER-BBN and Praxis Pharmaceuticals, TERARMET (RTC-2014-2207-1) project financed by MEC (Spain), and excellence Grant CTS-6270 financed by "Junta de Andalucía". The authors also wish to thank the Microscopy Service of UAB, especially Dr. Pablo Castro for the technical support in taking the Cryo-TEM images, Mª Eugenia López Sánchez and Natalia García Aranda for their technical assistance in the in vitro activity assays, and Amable Bernabé for its cooperation as technician of the Soft Materials Service linked to NANBIOSIS Biomaterial Processing and Nanostructuring Unit at ICMAB-CSIC . A.V. is recipient of an ICREA Academia (Generalitat de Catalunya) award. The authors acknowledge EMBL and Electra synchrotrons for beamtime allocation, and H. Amenitsch, B. Marmilori, and B. Sartori for technical support at the SAXS beamline. Access to the synchrotron facility was supported by the BioStructX program (no. BIOSTRUCTX_1093). The authors also acknowledge computer time at the Minotauro-BSC supercomputer from the Red Española de Supercomputación (RES).

Received: September 15, 2015
Revised: December 3, 2015
Published online:

[1] R. J. Desnick, R. Brady, J. Barranger, A. J. Collins, D. P. Germain, M. Goldman, G. Grabowski, S. Packman, W. R. Wilcox, *Ann. Intern. Med.* **2003**, *138*, 338.
[2] C. M. Eng, N. Guffon, W. R. Wilcox, D. P. Germain, P. Lee, S. Waldek, L. Caplan, G. E. Linthorst, R. J. Desnick, *New Engl. J. Med.* **2001**, *345*, 9.
[3] R. M. Schaefer, A. Tulki-Szymanska, M. J. Hilz, *Drugs* **2009**, *69*, 2179.
[4] A. Pisani, B. Visciano, G. D. Roux, M. Sabbatini, C. Porto, G. Parenti, M. Imbriaco, *Mol. Genet. Metab.* **2012**, *107*, 267.
[5] I. Y. Desnick RJ, in *The Metabolic and Molecular Bases of Inherited Disease*, Vol. *3* (Eds: C. R. Scriver, W. S. Sly, D. Valle), McGraw-Hill, New York **2001**, 3733.
[6] P. F. Bodary, J. A. Shayman, D. T. Eitzman, *Trends Cardiovasc. Med.* **2007**, *17*, 129.
[7] J. S. Shen, X. L. Meng, D. F. Moore, J. M. Quirk, J. A. Shayman, R. Schiffmann, C. R. Kaneski, *Mol. Genet. Metab.* **2008**, *95*, 163.
[8] T. Kizhner, Y. Azulay, M. Hainrichson, Y. Tekoah, G. Arvatz, A. Shulman, I. Ruderfer, D. Aviezer, Y. Shaaltiel, *Mol. Genet. Metab.* **2015**, *114*, 259.
[9] F. C. Fervenza, R. Torra, D. G. Warnock, *Biol. Targets Ther.* **2008**, *2*, 823.
[10] C. Siatskas, J. A. Medin, *J. Inherit. Metab. Dis.* **2001**, *24*, 25.
[11] M. I. Giannotti, O. Esteban, M. Oliva, M. F. Garcia-Parajo, F. Sanz, *Biomacromolecules* **2011**, *12*, 2524.
[12] S. H. Cheng, A. E. Smith, *Gene Ther.* **2003**, *10*, 1275.
[13] M. S. Sands, B. L. Davidson, *Mol. Ther.* **2006**, *13*, 839.
[14] R. A. Dwek, T. D. Butters, F. M. Platt, N. Zitzmann, *Nat. Rev. Drug Discov.* **2002**, *1*, 65.
[15] C. Porto, M. Cardone, F. Fontana, B. Rossi, M. R. Tuzzi, A. Tarallo, M. V. Barone, G. Andria, G. Parenti, *Mol. Ther.* **2009**, *17*, 964.
[16] J. Q. Fan, S. Ishii, *FEBS J.* **2007**, *274*, 4962.
[17] J. Hsu, D. Serrano, T. Bhowmick, K. Kumar, Y. Shen, Y. C. Kuo, C. Garnacho, S. Muro, *J. Control. Release* **2011**, *149*, 323.
[18] B. Heurtault, P. Saulnier, B. Pech, J. E. Proust, J. P. Benoit, *Biomaterials* **2003**, *24*, 4283.
[19] M. Chanana, P. Rivera-Gil, M. A. Correa-Duarte, L. M. Liz-Marzán, W. J. Parak, *Angew. Chem. Int. Ed.* **2013**, *52*, 4179.
[20] P. Rivera-Gil, S. De Koker, B. G. De Geest, W. J. Parak, *Nano Lett.* **2009**, *9*, 4398.
[21] M. Lundqvist, J. Stigler, G. Elia, I. Lynch, T. Cedervall, K. A. Dawson, *Proc. Natl. Acad. Sci. USA* **2008**, *105*, 14265.
[22] M. Lundqvist, *Nat. Nanotechnol.* **2013**, *8*, 701.
[23] D. Hühn, K. Kantner, C. Geidel, S. Brandholt, I. De Cock, S. J. H. Soenen, P. Rivera-Gil, J. M. Montenegro, K. Braeckmans, K. Müllen, G. U. Nienhaus, M. Klapper, W. J. Parak, *ACS Nano* **2013**, *7*, 3253.
[24] M. Cano-Sarabia, N. Ventosa, S. Sala, C. Patino, R. Arranz, J. Veciana, *Langmuir* **2008**, *24*, 2433.
[25] I. Cabrera, E. Elizondo, O. Esteban, J. Luis Corchero, M. Melgarejo, D. Pulido, A. Cordoba, E. Moreno, U. Unzueta, E. Vazquez, I. Abasolo, S. SchwartzJr., A. Villaverde, F. Abericio, M. Royo, M. F. Garcia-Parajo, N. Ventosa, J. Veciana, *Nano Lett.* **2013**, *13*, 3766.
[26] R. R. Sawant, V. P. Torchilin, *Soft Matter* **2010**, *6*, 4026.
[27] V. P. Torchilin, *AAPS J.* **2007**, *9*, E128.
[28] T. Kubo, T. Sugita, S. Shimose, Y. Nitta, Y. Ikuta, T. Murakami, *Int. J. Oncol.* **2000**, *17*, 309.
[29] N. Ventosa, J. Veciana, I. Cabrera, E. Elizondo, M. Melgarejo, M. Royo, F. Albericio, D. Pulido, S. Sala, J. L. Corchero, S. Schwartz, I. Abasolo, A. Villaverde, *WO2014/001509*, **2012**.
[30] D. M. Beauvais, B. J. Ell, A. R. McWhorter, A. C. Rapraeger, *J. Exp. Med.* **2009**, *206*, 691.
[31] J. H. Grubb, C. Vogler, W. S. Sly, *Rejuv. Res.* **2010**, *13*, 229.
[32] K. Utsumi, K. Itoh, R. Kase, M. Shimmoto, N. Yamamoto, Y. Katagiri, K. Tanoue, M. Kotani, T. Ozawa, T. Oguchi, H. Sakuraba, *Clin. Chim. Acta* **1999**, *279*, 55.
[33] J. L. Corchero, R. Mendoza, J. Lorenzo, V. Rodriguez-Sureda, C. Dominguez, E. Vazquez, N. Ferrer-Miralles, A. Villaverde, *Biotechnol. Prog.* **2011**, *27*, 1206.
[34] A. E. Nel, L. Mädler, D. Velegol, T. Xia, E. M. V. Hoek, P. Somasundaran, F. Klaessig, V. Castranova, M. Thompson, *Nat. Mater.* **2009**, *8*, 543.
[35] J. L. Corchero, R. Mendoza, N. Ferrer-Miralles, A. Montràs, L. M. Martínez, A. Villaverde, *Biochem. Eng. J.* **2012**, *67*, 20.
[36] B. J. Johnson, W. Russ Algar, A. P. Malanoski, M. G. Ancona, I. L. Medintz, *Nano Today* **2014**, *9*, 102.
[37] S. C. Garman, D. N. Garboczi, *J. Mol. Biol.* **2004**, *337*, 319.
[38] A. L. Lomize, I. D. Pogozheva, M. A. Lomize, H. I. Mosberg, *Protein Sci.* **2006**, *15*, 1318.
[39] S. Hatakeyama, K. Sugihara, T. K. Shibata, J. Nakayama, T. O. Akama, N. Tamura, S. M. Wong, A. A. Bobkov, Y. Takano, C. Ohyama, M. Fukuda, M. N. Fukuda, *Proc. Natl. Acad. Sci. USA* **2011**, *108*, 19587.
[40] E. Ruoslahti, S. N. Bhatia, M. J. Sailor, *J. Cell Biol.* **2010**, *188*, 759.
[41] Y. S. Haviv, J. L. Blackwell, A. Kanerva, P. Nagi, V. Krasnykh, I. Dmitriev, M. Wang, S. Naito, X. Lei, A. Hemminki, D. Carey, D. T. Curiel, *Cancer Res.* **2002**, *62*, 4273.
[42] R. J. Hopkin, J. Bissler, G. A. Grabowski, *Genet. Med.* **2003**, *5*, 144.

[43] Y. A. Ioannou, K. M. Zeidner, R. E. Gordon, R. J. Desnick, *Am. J. Hum. Genet.* **2001**, *68*, 14.
[44] A European Medicines Agency, *Reflection paper on the data requirements for intravenous liposomal products developed with reference to an innovator liposomal product. EMA/CHMP/806058/2009/Rev.02*, http://www.ema.europa.eu/ema/index.jsp?curl=pages/regulation/general/general_content_000564.jsp&mid=WC0b01ac05806403e0, **2013**.
[45] R. J. Desnick, K. Y. Allen, S. J. Desnick, M. K. Raman, R. W. Bernlohr, W. Krivit, *J. Lab. Clin. Med.* **1973**, *81*, 157.
[46] J. S. Mayes, J. B. Scheerer, R. N. Sifers, M. L. Donaldson, *Clin. Chim. Acta* **1981**, *112*, 247.
[47] L. Shu, H. S. Murphy, L. Cooling, J. A. Shayman, *J. Am. Soc. Nephrol.* **2005**, *16*, 2636.
[48] W. Humphrey, A. Dalke, K. Schulten, *J. Mol. Graph.* **1996**, *14*, 33.
[49] R. Feynman, *Eng. Sci.* **1960**, *23*, 22.